SECOND EUROPEAN CONFERENCE ON EARTHQUAKE ENGINEERING AND SEISMOLOGY, ISTANBUL AUG. 25-29, 2014

DYNAMIC PROPERTIES CHANGE OF SOIL-STRUCTURE INTERACTION OF SRC BUILDING BEFORE AND AFTER THE 2011 OFF THE PACIFIC COAST OF TOHOKU EARTHQUAKE

Koichi MORITA[1] and Toshihide KASHIMA[2]

ABSTRACT

In this paper, the identification of the dynamic properties of soil-structure interaction on an existing eight-storey steel-encased reinforced concrete building is shown through strong motion observations. An identification method for the soil-structure interaction stiffness, in which only the natural frequency and mass values are utilized, is proposed. By applying this method to strong motion data, the soil-structure interaction stiffness can be estimated.

INTRODUCTION

In order to reduce life cycle costs of a building from construction to maintenance, it is very effective to monitor the structural health of a building. Recently, there are many researches on identification and evaluation for natural frequency, damping ratio and stiffness of existing buildings through strong motion observation or microtremor observation from the viewpoint of the structural health monitoring. In such estimation through measurement, the horizontal motion of ground floor or basement floor is assumed as input motion and horizontal motion of building as response motion. The effect of soil-structure interaction is not enough considered.

On the other hand, in middle-to-low rise buildings the effect of soil-structure interaction affects the vibration characteristic of the building. The effect to vibration characteristic of the building by soil-structure interaction is discussed in some researches, but the example of identifying ground stiffness of the interaction system is very little. (Stewart and Fenves, 1998) There is a research on identifying ground stiffness of the interaction system by a technique which resembled based on the simple Penzien model (Penzien et al., 1964) for the building with the pile foundation. (Choi and Hamamoto, 2010) This method is complicated because the unknown parameter are gradually obtained by the curved fitting.

In the other, parametric identification techniques which has good accuracy are recently proposed. The application of these methods is simple and it seems to be a simple method, if identification technique of ground stiffness of the interaction system uses these identification results.

In this study, we identified the natural frequencies using seismic observation data for an eight-story steel-encased reinforced concrete building (Kashima and Kitagawa, 2004) for which continuous seismic observation had been made since the completion of construction. We focused on the influence of soil-structure interaction on the natural frequencies of the building and evaluated the natural frequencies with consideration given to the influence of the interaction. We also analysed the structural age and amplitude dependence.

[1] Head, National Institute for Land and Infrastructure Management, Tsukuba, morita@kenken.go.jp
[2] Senior Research Engineer, Building Research Institute, Tsukuba, kashima@kenken.go.jp

Furthermore, simple identification technique of the ground stiffness of soil-structure interaction system using the natural frequencies which the dynamic interaction influenced is proposed. This technique is applied to strong-motion record data of an existing building, and the dependence of structural age and amplitudes of ground stiffness is analysed.

BUILDING DESCRIPTION AND INSTRUMENTATION

The target building is the Research Center for Disaster Risk Management of the National Institute for Land and Infrastructure Management, Ministry of Land, Infrastructure, Transport and Tourism (completed in March 1998) and an overview of the building is shown in Table.1. A strong-motion seismograph system was installed immediately after the completion of the construction and observation has been continued since then. Accelerometers were installed on the nearby surface ground, the first basement level, the first floor, the second floor, the fifth floor, and the eighth floor shown as Fig. 1. Among the data provided by these sensors, we used only data of the sensors on the subsurface ground, the first basement level, and the eighth floor.

From the strong motion records until now, we use only the strong motion data in which peak ground acceleration is over 20cm/s2.

The results of ground survey carried out in the installation of the observation system is shown at Table.2.

Table 1. Overview of building

Building name	Research Center for Disaster Risk Management of National Institute for Land and Infrastructure Management
Number of floors	Eight stories with one basement floor
Floor area	5,050 m^2
Height	30.9 m
Embedded depth	8.2 m
Main structure	Steel-encased reinforced concrete
Foundation structure	Spread foundation

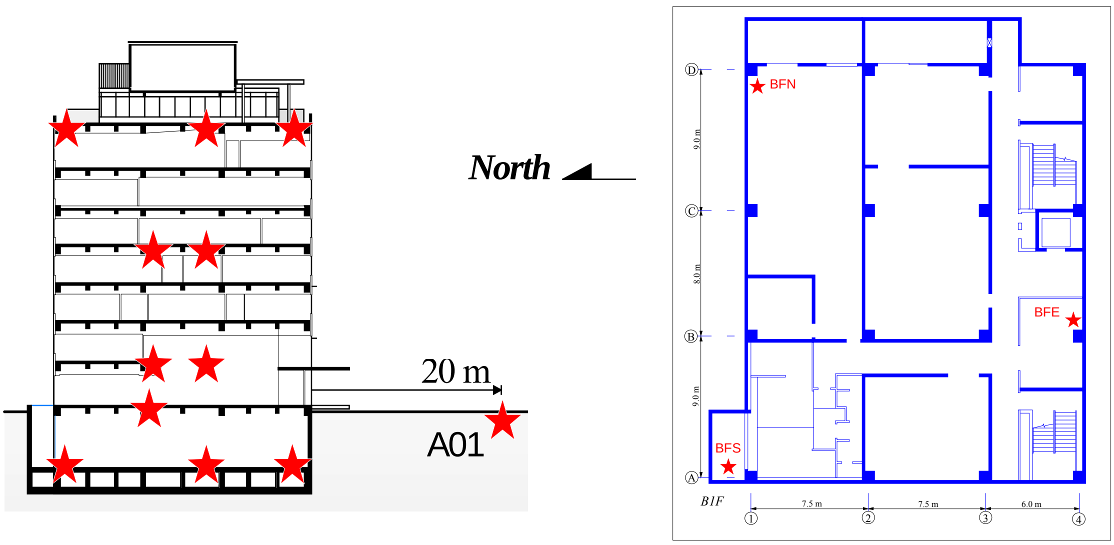

Figure 1. Building and installation locations of strong-motion accelerometers

Table 2. Soil structure

No.	Thickness (m)	VP (m/s)	Vs (m/s)	ρ (t/m^3)	soil property
1	2.0	170	110	1.30	loam layer
2	6.0	1430	200	1.30	sandy clay / clayey sand
3	6.0		160	1.50	sandy clay / clay
4	8.0	1630	260	1.80	fine sand / sandy fine sand
5	6.0	1500	200	1.75	sandy clay / clay
6	14.0	1570	270		
7	6.0	1880	460	1.90	sand gravel
8	8.0	1780	340	1.75	sandy clay / clay
9	12.0	1690	290		
10	12.0	1790	380	1.95	sand gravel / fine sand
11	8.0	1600	280	1.75	sandy clay /clay
12			500	2.00	sand gravel

IDENTIFICATION METHOD APPLIED

Acceleration records of input and response on the eighth floor were used to identify damping ratios by the system identification approach. As the identification method itself can cause variations, the ARX model (Ljung, 1987), which can provide relatively accurate calculation of natural frequencies to earthquake motion data, was used to identify parameters. The equation for the ARX model is as shown below:

$$y(t) + a_1 y(t-1) + ... + a_{n_a} y(t-n_a) = b_1 u(t-n_k) + ... + b_{n_b} u(t-n_k-n_b+1) \tag{1}$$

This equation relates current output (*y(t))* to the limited numbers of past output data (*y(t-k))* and input data (*u(t-k))*. In (1), n_a is the number of poles; n_{b-1} is the number of zeros; and n_k is dead time. According to the identification by ARX, model structure coefficients a_j and b_j are estimated. *A(q)* shown below is defined as the polynomial equation of irreducible shift parameter (*q*).

$$A(q) = 1 + \sum_{j=1}^{n_a} a_j q^{-j} \tag{2}$$

In Eqn.(2), $_zp_j$ is the root of *A(z)=0*. Then, the natural frequency is calculated as follows (Saito et al., 2005):

$$f_j = \frac{\sqrt{(\log|_z p_j|)^2 + (\arg{}_z p_j)^2}}{2\pi\Delta t} \tag{3}$$

It is recommended that model orders be determined by AIC (Akaike's Information Criterion: Index to measure goodness-of-fit of a model obtained from the maximum likelihood estimation method) (Akaike, 1974), etc., so we select the numbers in which AIC is estimated as minimum.

THREE TYPES OF NATURAL FREQUENCIES DETERMINED IN THIS STUDY

Data from the accelerometers shown in Fig. 1 were used to determine natural frequencies and the following three types of natural frequencies with consideration of the influence of the interaction were determined:

1) Combined system, including horizontal motion and rotational motion of the foundation: Natural frequency of SRB type; T_{SRB}
(Input: Acceleration of the ground surface 20 m away from the building; $\ddot{Z}$ in Fig. 2)
2) Upper deformation + rotational motion: Natural frequency of RB type; T_{RB}
(Input: Acceleration of the first basement level; $\ddot{x}_S + \ddot{Z}$ in Fig. 2)
3) Fixed-base system of building deformation only: Natural frequency of B type; T_B
(Input: Acceleration of the first basement level + rotational motion of the foundation; $H\ddot{\theta} + \ddot{x}_S + \ddot{Z}$ in Fig. 2)

For 3), vertical motions on the first basement level (two locations) were used. Responses represent the acceleration on the eighth floor for all the three cases; $\ddot{x}_T + \ddot{Z}$ in Fig. 2. Natural frequencies determined from the input-output relationships respectively in 1), 2), and 3) are hereafter called the SRB-type natural frequency, the RB-type natural frequency, and the B-type natural frequency.

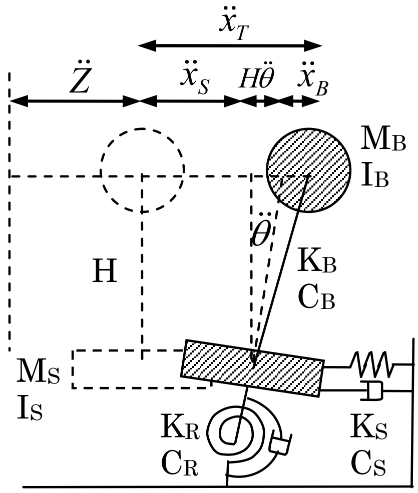

Figure 2. Input and response in the sway-rocking model

IDENTIFICATION METHOD OF THE GROUND STIFFNESS OF SOIL-STRUCTURE INTERACTION SYSTEM

Damping ratio of the target building is about 2-5%. In the following calculation, natural frequency is assumed as undamped mode natural frequency. The equation of motion of base fixed single-degree-of-freedom system shown as Fig. 2 is expressed as following;

$$M_B\ddot{x} + C_B\dot{x} + K_B x = -M_B\ddot{z} \tag{4}$$

where M_B, K_B, and C_B are mass, stiffness, and damping coefficient of building. Then, the circular frequency in the undamped mode is ω_B and

$$K_B = \omega_B{}^2 M_B \tag{5}$$

The stiffness of building is determined as above.

The equation of motion for the single-degree-of-freedom system with consideration of rocking in Fig. 2 is expressed as

$$\begin{bmatrix} I & 0 \\ HM_B & M_B \end{bmatrix}\begin{Bmatrix} \ddot{\theta} \\ \ddot{x} \end{Bmatrix} + \begin{bmatrix} C_R & -C_B H \\ 0 & C_B \end{bmatrix}\begin{Bmatrix} \dot{\theta} \\ \dot{x}_B \end{Bmatrix} + \begin{bmatrix} K_R & -K_B H \\ 0 & K_B \end{bmatrix}\begin{Bmatrix} \theta \\ x_B \end{Bmatrix} = \begin{Bmatrix} 0 \\ -M_B \ddot{z} \end{Bmatrix}, \tag{6}$$

where K_R and C_R are stiffness and damping coefficient of rocking and

$I = I_B + I_S$: rotary inertia

H: equivalent height of building.

When circular frequency in the undamped mode is expressed as ω_{RB} ,

$$\left| -\omega_{RB}{}^2 \begin{bmatrix} I & 0 \\ M_B H & M_B \end{bmatrix} + \begin{bmatrix} K_R & -K_B H \\ 0 & K_B \end{bmatrix} \right| = 0 \tag{7}$$

Therefore,

$$K_R = \frac{(K_B I + K_B M_B H^2)\omega_{RB}{}^2 - I M_B \omega_{RB}{}^4}{K_B - M_B \omega_{RB}{}^2} \tag{8}$$

The stiffness of rocking is determined as above. When calculating stiffness by Eq. (8), rotary inertia I and identified natural frequency f_{RB} are used.

The equation of motion for the single-degree-of-freedom system with consideration of rocking and sway in Fig. 2 is expressed as

$$\begin{bmatrix} I & 0 & 0 \\ 0 & M_S & 0 \\ M_B H & M_B & M_B \end{bmatrix}\begin{Bmatrix} \ddot{\theta} \\ \ddot{x}_S \\ \ddot{x}_B \end{Bmatrix} + \begin{bmatrix} C_R & 0 & -C_B H \\ 0 & C_S & -C_B \\ 0 & 0 & C_B \end{bmatrix}\begin{Bmatrix} \dot{\theta} \\ \dot{x}_S \\ \dot{x}_B \end{Bmatrix} + \begin{bmatrix} K_R & 0 & -K_B H \\ 0 & K_S & -K_B \\ 0 & 0 & K_B \end{bmatrix}\begin{Bmatrix} \theta \\ x_S \\ x_B \end{Bmatrix} = \begin{Bmatrix} 0 \\ -M_S \ddot{z} \\ -M_B \ddot{z} \end{Bmatrix} \tag{9}$$

where K_S and C_S are stiffness and damping coefficient of sway and

M_S: Mass at basement

When circular frequency in the undamped mode is expressed as ω_{SRB} ,

$$\left| -\omega_{SRB}{}^2 \begin{bmatrix} I & 0 & 0 \\ 0 & M_S & 0 \\ M_B H & M_B & M_B \end{bmatrix} + \begin{bmatrix} K_R & 0 & -K_B H \\ 0 & K_S & -K_B \\ 0 & 0 & K_B \end{bmatrix} \right| = 0 \tag{10}$$

Therefore,

$$K_S = \frac{\omega_{SRB}^2 M_S(-\omega_{SRB}^2 I + K_R)(-\omega_{SRB}^2 M_B + K_B) - \omega_{SRB}{}^4 M_B H^2 K_B + (-\omega_{SRB}^2 I + K_R)\omega_{SRB}^2 K_B M_B}{(-\omega_{SRB}^2 I + K_R)(-\omega_{SRB}^2 M_B + K_B) - \omega_{SRB}{}^2 M_B H^2 K_B} \tag{11}$$

The stiffness of sway is determined as above. When calculating stiffness by Eq. (11), Mass Ms and identified natural frequency f_{SRB} are used.

In this method, ground stiffness of soil-structure interaction can be determined by only using three natural frequencies, if mass, rotary inertia and equivalent height are given. Therefore, identification accuracy of ground stiffness is greatly dependent on identification accuracy of natural frequencies. It is necessary to use the identification technique of the natural frequency which the accuracy is higher. In this paper, parameter identification method by the ARX model has been utilised.

From Eqns.(5) and (8),

$$K_R = \omega_{RB}^2 \frac{I + M_B H^2 - I\left(\dfrac{\omega_{RB}}{\omega_B}\right)^2}{1 - \left(\dfrac{\omega_{RB}}{\omega_B}\right)^2} \tag{12}$$

From this equation, evaluated stiffness tends to rapidly increase, when ratio of the natural frequencies is almost 1. The small error of identified natural frequencies can influence the rocking stiffness.

APPLICATION TO SIMULATION WAVE

In order to verify identification method shown at previous chapter, we compare the set value with the identified value from response wave by inputting white noise into the SR mode. SR model of an analysis target is assumed as building of research center for disaster risk management of national institute for land and infrastructure management. That is to say, the superstructure of the building is assumed as multi-degree-of-freedom system model, and story mass and story stiffness is based on the construction plan document of the building and push-over analysis was carried out. Story mass and stiffness are shown in Table. 3, and equivalent height and equivalent mass which is abbreviated as single-degree-of-freedom system are shown in Table. 4. The mode shape is assumed to be the inverted triangle in abbreviating as single-degree-of-freedom system. First damping ratio of the superstructure is set to be 2%, and higher mode is made to be initial stiffness proportional. The stiffness of rocking and sway is calculated by the simple method which uses the cone model for the elasticity theory solution of the uniform ground by using the soil-structure of Table. 2. Damping coefficient of rocking and sway are given by practical equation of Parmelee. (Parmelee. 1970) Values of the setting model are shown at Table. 5.

Table 3. Mass and stiffness of building

story	mass[kg]	stiffness[N/m]
7	1.118E+06	7.404E+08
6	7.438E+05	1.053E+09
5	7.673E+05	1.183E+09
4	9.310E+05	1.260E+09
3	7.820E+05	1.458E+09
2	7.850E+05	2.405E+09
1	8.359E+05	1.167E+10

Table 4. Equivalent height and equivalent mass of single-degree-of-freedom system

equivalent height	H	1.983E+01	[m]
equivalent mass	M_B	4.830E+06	[kg]

Table 5. Setting values of SR model

rotary inertia	I	3.360E+08	[kg・m^2]
Mass at basement	M_S	1.262E+06	[kg]
Rocking stiffness	K_R	1.232E+12	[N・m]
Sway stiffness	K_S	5.434E+09	[N/m]
Rocking damping coefficient	C_R	1.352E+09	[N・s・m]
sway damping coefficient	C_S	1.211E+08	[N・s/m]

The response analysis is carried out by using the model shown at Tables 3 and 5. Identification method by the ARX model is applied to simulation wave, and natural frequencies shown at Table. 6 are obtained. The stiffness of rocking and sway which is calculated from three natural frequencies by using rotatory inertia, equivalent mass and equivalent height shown in Table. 4 is shown at Table. 7. It was proven that by this, stiffness of rocking are sway is identified in good accuracy.

Table 6. Identified natural frequencies

f_B	1.512[Hz]
f_{RB}	1.414[Hz]
f_{SRB}	1.371[Hz]

Table 7. Identified stiffness

	Identified value	Setting value
K_R[N･m]	1.216E+12	1.232E+12
K_S[N/m]	6.298E+09	5.434E+09

In the example above, f_{SRB}/f_B is about 0.91 and f_{RB}/f_B is about 0.93. In some cases, f_{RB}/f_B and f_{SRB}/f_B are almost 1 for the target building as shown in the following chapter. Simulation waveform is calculated by using the result of sway and rocking stiffness shown in Table. 8 in order to examine the example in which f_{RB}/f_B and f_{SRB}/f_B are almost 1.

Table 8. Changed stiffness of rocking and sway

Rocking stiffness	K_R	4.000E+12	[N･m]
Sway stiffness	K_S	2.000E+10	[N/m]

Identified results of natural frequencies and stiffness are shown in Tables 9 and 10. From these tables, stiffness of rocking and sway can be identified in good accuracy even if f_{RB}/f_B and f_{SRB}/f_B are almost 1.

Table 9. Identified natural frequencies

f_B	1.512 [Hz]
f_{RB}	1.480 [Hz]
f_{SRB}	1.466 [Hz]

Table 10. Identified stiffness

	Identified value	Setting value
K_R[N･m]	3.948E+12	4.000E+12
K_S[N/m]	2.225E+10	2.000E+10

IDENTIFICATION RESULTS

Examples of spectral ratio of strong motion are shown in Figs. 3 and 4. In Fig.3 in which strong motion was recorded just after the completion of building (1999.04.25), the position of three peaks is difference. In Fig. 4 in which strong motion was recorded after the 2011 off the Pacific coast of Tohoku Earthquake (2012.01.01), the position of three peaks is almost same and natural frequencies of the system decreased very much.

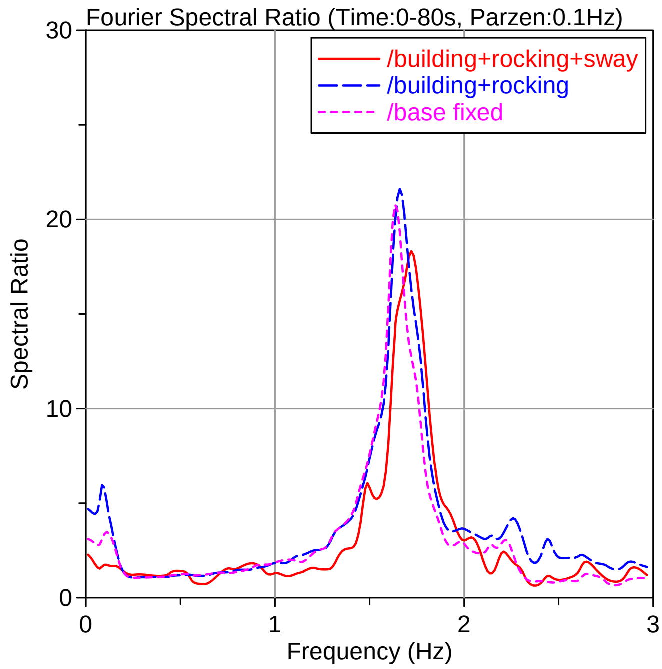

Figure 3. Spectral ratio of strong motion (1999.04.25)

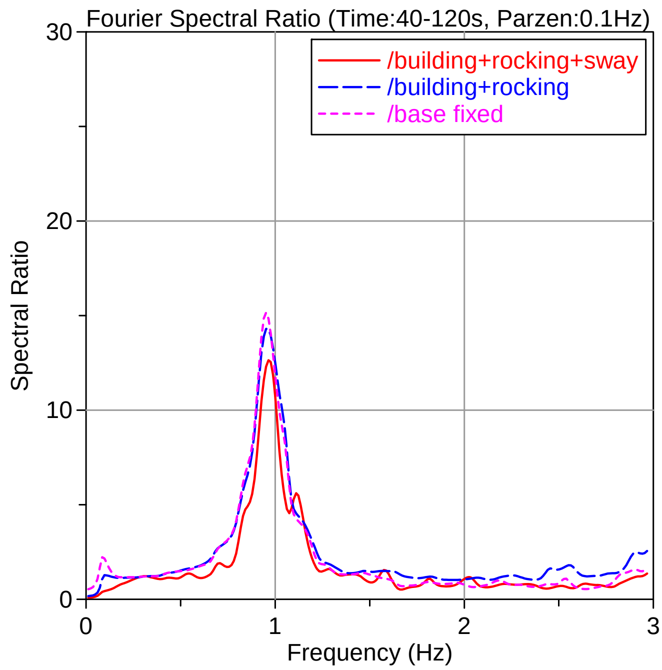

Figure 4. Spectral ratio of strong motion (2012.01.01)

The three types of natural frequencies were determined for the strong motion observation records (for the whole duration) whose GPA is larger than 20cm/sec^2 and their relationship with structural age are shown in Fig. 5. Natural frequencies tend to decrease after completion of the building and after 7 years of completion they are almost constant. After the 2011 off the pacific coast of Tohoku earthquake, natural frequencies drop to about 1.0Hz. The natural frequencies do not restore till now. The magnitude relationships of three types natural frequencies are $f_B > f_{BR} > f_{SRB}$ in all cases. The cause of lowering natural frequencies in Fig. 5 is due to the characteristics change of superstructure, and lowering stiffness of superstructure comes from small crack of non-structural wall and structural wall contribution change of non-structural members. Fig. 6 shows the ratio between two natural frequencies calculated by dividing SRB-type and RB-type natural frequencies by the B-type natural frequency. According to this figure, the ratio between the two frequencies tends to increase with structural age. Just after completion of the building, the ratio between the two frequencies is 0.92-0.94 and after the 2011 off the Pacific coast of Tohoku Earthquake the ratio is 0.97-0.99. The cause of ratio between two natural frequencies is in change of rocking stiffness, and tendency rocking stiffness are shown in next page.

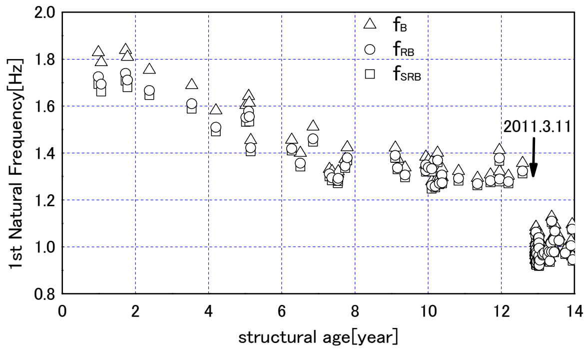

Figure 5. Structural age dependence of natural frequencies

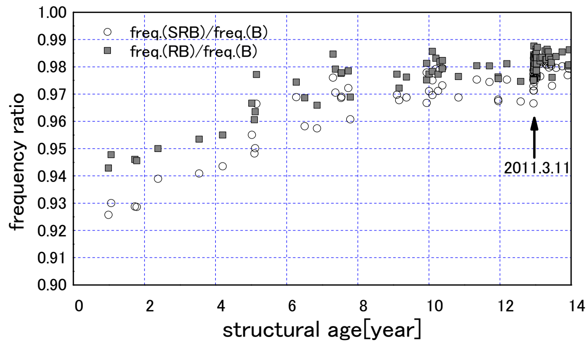

Figure 6. Structural age dependence of natural frequency ratio

Building stiffness, rocking stiffness and sway stiffness are estimated by using the values shown in Table 11. The relationship with structural age and rocking stiffness are shown in Figure 7. The rocking stiffness tends to increase with structural age, although variability is seen. As the reason why the dispersion of identification value after 4 years, negligible identification error of natural frequencies seems to influence identification value of rocking stiffness when frequency ratio (f_{RB}/f_B) shown in Fig. 6 is almost 1. The rocking stiffness largely decreased after the 2011 off the pacific coast of Tohoku earthquake. The rocking stiffness do not restore till now. Based on visual inspection, no ground deformation was observed around this building. In Figure 8, sway stiffness has large variation when natural frequency ratio is almost 1.0, but stiffness value tends to be smaller just after the 2011 off the pacific coast of Tohoku earthquake. The relationship between peak ground acceleration and rocking stiffness is shown Fig. 9. The value varies before the 2011 off the pacific coast of Tohoku earthquake, and the value tends to be smaller in larger acceleration after the 2011 off the pacific coast of Tohoku earthquake.

Table 11. Values used for identification

equivalent height of building	H	1.983E+01	[m]
equivalent mass of building	M_B	4.830E+06	[kg]
rotary inertia	I	3.360E+08	[kg･m^2]
mass of basement	M_S	1.262E+06	[kg]

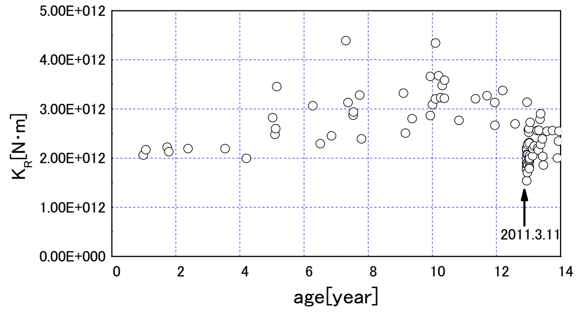

Figure 7. Structural age dependence of rocking stiffness

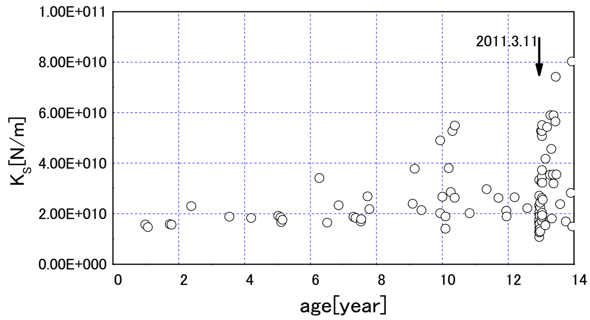

Figure 8. Structural age dependence of sway stiffness

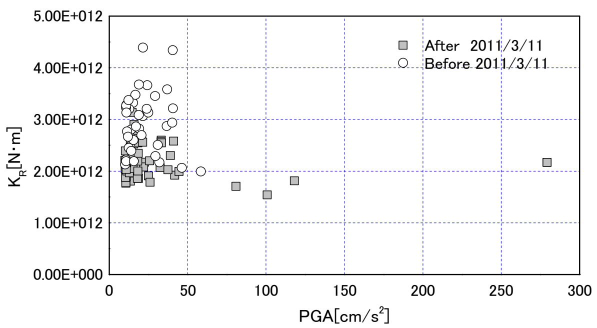

Figure 9. Amplitude dependence of rocking stiffness

CONCLUSIONS

Simple identification method of ground stiffness of soil-structure interaction system using natural frequencies and known mass values etc. was proposed. We determined the ground stiffness using strong motion observation data of an existing building. As a result of evaluating dynamic characteristics with consideration given to the influence of soil-structure interaction, we obtained the following findings within the scope of this study:

1) It is proven that ground stiffness of soil-structure interaction system can be identified by this technique at good accuracy in the application to simulated wave.
2) Three types of natural frequencies tend to decrease for the first seven years and greatly decrease after the Tohoku earthquake. The natural frequencies do not restore till now.

3) The natural frequency ratio dividing by B type natural frequency tends to increase with structural age, and a little bit increase after the Tohoku earthquake.
4) The rocking stiffness tends to increase with structural age and largely decreased after the Tohoku earthquake.
5) The sway stiffness has large variation when natural frequency ratio is almost 1.0, but stiffness value tends to be smaller just after the Tohoku earthquake.

REFERENCES

Akaike H (1974). "A new look at the statistical model identification", *IEEE Transactions on Automatic Control* **19:6**, 716–723.

Choi J and Hamamoto T (2010). "Shaking Table Test on Indirect Health Monitoring of Pile Foundation", *Proc. 5th World Conference on Structure Control Monitoring*, 5WCSCM-081

Kashima T and Kitagawa Y (2004). "Dynamic Behaviour Of An Eight-Storey SRC Building Examined From Strong Motion Records", *13th World Conference on Earthquake Engineering*, Paper No.196.

Ljung L (1987). System Identification, Prince Halls, NJ.

Parmelee RA (1970). "The Influence of Foundation Parameters on the Seismic Response of Interaction Systems", *Proc. Third Japan Earthquake Symposium*, 49-56

Penzien J, Scheffey CF and Parmelee RA (1964) "Seismic. Analysis of Bridges Long Piles", *J. of the Eng. Mech. Div., Proc. of ASCE*, **90**, No.EM3, 223-254

Saito T, Mase S and Morita K (2005). "A probabilistic approach to structural damage estimation", *Journal of Structural Control and Health Monitoring* **12**, 283-299.

Stewart JP and Fenves GL (1998). System Identification for Evaluating Soil-Structure Interaction Effects in Buildings from Strong Motion, *Earthquake Engineering and Structural Dynamics* **27,** 869-885